

A&A manuscript no.  
(will be inserted by hand later)

Your thesaurus codes are:  
05(10.07.3  $\omega$  Cen, NGC6397, NGC6752, Liller 1, 13.25.5)

ASTRONOMY  
AND  
ASTROPHYSICS

# Multiple and variable X-ray sources in the globular clusters $\omega$ Cen, NGC 6397, NGC 6752, and Liller 1

F. Verbunt<sup>1</sup> and H.M. Johnston<sup>2</sup>

<sup>1</sup> Astronomical Institute, P.O.Box 80000, NL-3508 TA Utrecht, The Netherlands

<sup>2</sup> Anglo Australian Observatory, P.O. Box 296, Epping, NSW 2121, Australia

November 24, 2018, accepted

**Abstract.** We detect stars from the Hipparcos and Tycho Catalogues in the field of view of observations with the ROSAT HRI of three globular clusters. We use the positions of these stars to reduce the systematic error in the positions of X-ray sources in the clusters to  $\sim 2''$  for  $\omega$  Cen and NGC 6752, and  $1''$  for NGC 6397. We detect three X-ray sources in the core of  $\omega$  Cen, and four in the core of NGC 6752; the data for the center of NGC 6397 may be fitted with five or six sources. Outside the cores, but within the half-mass radius of the clusters, we detect two sources in  $\omega$  Cen, one in NGC 6397 and two in NGC 6752; these may or may not be cluster members. A ROSAT HRI observation of Liller 1 does not detect a low-luminosity source, at a limit below a detection with ASCA. We discuss the nature of the low-luminosity X-ray sources in globular clusters in the light of these new results.

**Key words:** globular clusters: individual  $\omega$  Cen, NGC 6397, NGC 6752, Liller 1 – X-rays: stars

## 1. Introduction

Globular clusters contain many X-ray sources at lower luminosities,  $L_x \lesssim 10^{34}$  erg s<sup>-1</sup>. These sources were first discovered with the Einstein satellite (Hertz & Grindlay 1983), and many more were found with ROSAT (for a compilation, see Johnston & Verbunt 1996). The nature of these low-luminosity sources is the subject of debate, because various types of objects can emit X-rays at such luminosities, such as soft X-ray transients in quiescence, cataclysmic variables, RS CVn binaries, and recycled neutron stars (see e.g. Fig. 8 in Verbunt et al. 1997). The most compelling identification of a dim X-ray source with an object observed at other wavelengths is the recycled radio pulsar in M 28: the X-ray flux varies on the pulse period (Danner et al. 1994). Plausible identifications with cataclysmic variables have been suggested for dim X-ray sources in NGC 6397, NGC 6752, NGC 5904 and 47 Tuc

(Cool et al. 1995b, Grindlay 1993, Hakala et al. 1997, Verbunt & Hasinger 1998). These identifications are based on the proximity of the X-ray position to that of a cataclysmic variable, and thus their probability depends on the accuracy of the X-ray position.

The accuracy of the ROSAT position of a detected X-ray source is determined by two factors: the statistical accuracy of the position of the source on the detector, and the accuracy with which the position of the detector as a whole is projected on the sky. For a sufficient number of photons the statistical error is less than an arcsecond, but the projection in general has a typical error of  $\sim 5''$ . Secure identification of a source in the detector field reduces the error in the projection to the statistical error of the identified source, provided that the optical (or radio) position has better accuracy. Only one identification is necessary, because the roll angle of the detector (i.e. the North-South direction) is accurately known; nonetheless, identification of more than one source is preferable to allow checks on internal consistency. In a globular cluster the surface density of possible counterparts is so high that chance coincidence usually cannot be excluded; a secure identification can usually be made only for X-ray sources detected well outside the cluster. This method has been used by Verbunt & Hasinger (1998) to improve the positional accuracy of the sources in the core of 47 Tuc from  $5''$  to  $2''$ , whereby the area in which the source is expected to lie is reduced sufficiently to exclude several proposed identifications, and increase the probability of others, including two possible cataclysmic variables.

In this paper we investigate three clusters known to contain multiple dim X-ray sources in their core, which have been observed in long exposures with the ROSAT HRI, and one cluster known to harbour a transient. We analyse hitherto unpublished observations and detect both previously published and new X-ray sources. All source positions are checked in the SIMBAD data base versus positions of other objects, and we find objects in the Hipparcos or Tycho Catalogues (ESA 1997, Perryman et al. 1997, Høg et al. 1997) with each cluster, i.e. counterparts with

**Table 1.** Log of the ROSAT HRI observations of globular clusters analysed in this paper. For each cluster observation, the observation date(s) and exposure time are given. We further give the shift in  $\alpha$ ,  $\delta$  applied to bring the X-ray coordinate frame of the longest observation to the optical coordinate frame J2000.

		observing period	$t_{\text{exp}}(\text{s})$	$\Delta\alpha$	$\Delta\delta$
		$\omega$ Cen			
1992	Aug	2448835.935–837.027	3469		
1993	Jan	2449008.688–008.702	1243		
1994	Jul	2449547.617–550.695	5997		
1995	Jan	2449735.780–744.786	17653		
1995	Jul	2449912.812–941.103	75481	$-0^{\circ}.05$	$0''0$
1996	Feb	2450120.247–130.418	12990		
1997	Jan	2450461.343–461.358	1317		
		NGC 6397			
1991	Mar	2448338.820–340.054	7499		
1992	Mar	2448696.631–697.646	12958		
1995	Mar	2449793.872–810.440	77204	$+0^{\circ}.11$	$-0''4$
		NGC 6752			
1992	Mar	2448697.719–703.626	31300	$-0^{\circ}.66$	$-1''3$
1995	Mar	2449800.941–815.431	17411		
1996	Apr	2450182.957–186.041	23278		
		Liller 1			
1996	Sep	2450332.541–337.810	16412		

describe the results for  $\omega$  Cen, NGC 6397, and NGC 6752, respectively. In Sect. 6 we discuss an observation of Liller 1. A discussion of our results is given in Sect. 7.

## 2. Observations and data reduction

The X-ray observations were obtained with the ROSAT X-ray telescope (Trümper et al. 1991) in combination with the high-resolution imager (HRI, David et al. 1995). The list of the observations is given in Table 1. The standard data reduction was done with the Extended Scientific Analysis System (Zimmermann et al. 1996), as follows. To take into account the re-calibration of the pixel size (Hasinger et al. 1998), we multiply the  $x, y$  pixel coordinates of each photon with respect to the HRI center with 0.9972. A search for sources is made by comparing counts in a box with the counts in a ring surrounding it, and by moving this detection box across the image. The sources thus detected are excised from the image and a background map is made for the remaining photons. A search for sources is then made by comparing the number of photons in a moving box with respect to the number expected on the basis of the background map. Finally, at each position in which a source was found, a maximum-likelihood technique is used to compare the observed photon distribution with the point spread function of the HRI (Crudace et al. 1988). This produces a maximum-likelihood value ML such that the probability that the source is due

sure that all such sources are found, we enter in the maximum likelihood technique all sources that have  $\text{ML} \geq 10$  according to the sliding box searches.)

Upper limits at the position of known sources were determined by counting the number  $n$  of actually detected photons at the position of the source (and in an area surrounding it corresponding to the uncertainty in the position); we then assign as upper limit the lowest expected number  $m$  for which the probability of measuring a number  $n$  or smaller is less than 5% according to the Poisson distribution.

The maximum-likelihood technique also provides an indication whether the source is extended. If such indication is present, we apply further analysis to test whether the source is a multiple point source.

The further analysis is also based on maximum likelihood techniques, but the analysis is limited to a small area of the detector, near its center. This allows the simplifications that the background in the analysed area is a constant (as opposed to a polynomial function of the  $x, y$  pixel coordinates), and that the point spread function is that for the center of the image (David et al. 1995). Suppose that a model to be tested predicts  $m_i$  photons at detector pixel  $i$ . The probability that  $n_i$  photons are observed is then given by the Poisson probability:

$$P_i = \frac{m_i^{n_i} e^{-m_i}}{n_i!} \quad (1)$$

The probability that the model describes the observations is given by the product of the probabilities for all  $i$  in the region considered:  $L' = \prod P_i$ . For computational ease we maximize the logarithm of this quantity:

$$\ln L' \equiv \sum_i \ln P_i = \sum_i n_i \ln m_i - \sum_i m_i - \sum_i \ln n_i! \quad (2)$$

The last term in this equation doesn't depend on the assumed model, and – in terms of selecting the best model – may be considered as a constant. Thus maximizing  $L'$  is equivalent to minimizing  $L$ , where

$$\ln L \equiv -2 \left( \sum_i n_i \ln m_i - \sum_i m_i \right) \quad (3)$$

If one compares two models A and B, with number of fitted parameters  $n_A$  and  $n_B$  and with likelihoods of  $\ln L_A$  and  $\ln L_B$ , respectively, the difference  $\Delta L \equiv \ln L_A - \ln L_B$  is a  $\chi^2$  distribution with  $n_A - n_B$  degrees of freedom, for a sufficient number of photons (Cash 1979, Mattox et al. 1996).

Our analysis of possibly multiple sources thus proceeds as follows. First we compute  $\Delta L$  for a model with constant background and for the best model with background plus one source, and compare it with the  $\chi^2$ -distribution with 3 degrees of freedom. If  $\Delta L > 15$ , the presence of one source has a significance more than three sigma. Next we compare

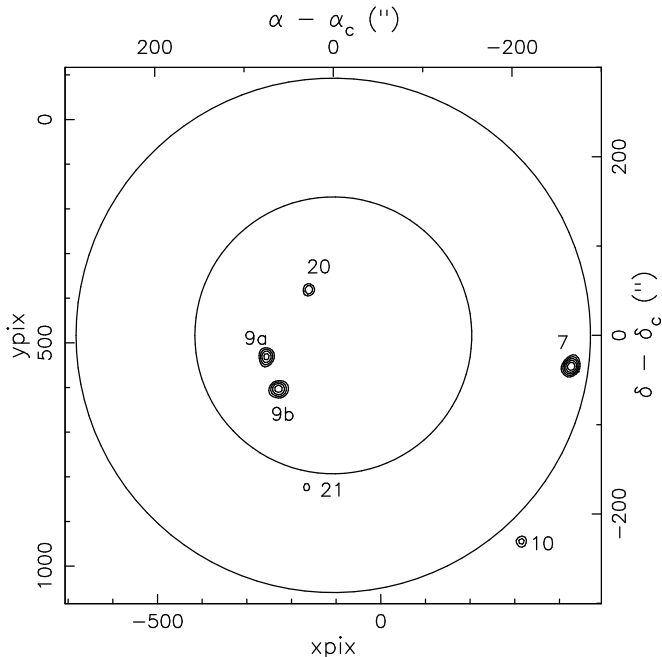


**Fig. 1.** X-ray contours in the central area of  $\omega$  Cen as observed with the ROSAT HRI in 1995 July. The image was smoothed with a 2-d  $\sigma \approx 5''$  Gaussian. The detected sources are indicated with their numbers in Table 2. The inner circle gives the core radius of the cluster, the outer circle the half-mass radius. The lower and left axes give pixel numbers for the ROSAT HRI detector, the upper and right axes right ascension and declination with respect to the cluster center. The conversion between pixel and celestial coordinates is accurate to within  $2''$ .

the best models with three and two sources to prove the significance of a third source, etc. until no more significant sources are found.

The addition of one source adds three fitted parameters, one for its number of counts and two for its position. In the case of NGC 6397 optical counterparts have been suggested for three X-ray sources. For these we also make a fit in which the distances in right ascension and declination between these three sources is fixed to the optically determined values. The three sources in that case only add five fitted parameters, two for the position of one of them, and three for the fluxes.

To determine the error in a parameter, we start from the best fit value  $a_i$ . We then fix the parameter at  $a_i + d$  and make a new fit, allowing all other parameters to vary. The value of  $d$  for which  $\ln L$  increases by 1 is quoted as the 1-sigma error.

### 3. $\omega$ Cen

$\omega$  Cen is a very massive globular cluster, with a relatively

**Table 2.** X-ray sources detected in the globular cluster  $\omega$  Cen ( $A_V = 0.47$ ,  $d = 4.9$  kpc, Djorgovski 1993) with the ROSAT HRI. Sources with a number less than 17 correspond to sources detected previously with the ROSAT PSPC (Johnston et al. 1994); those with a higher number are new sources. For each source we give the position, the statistical error in the position (in  $''$ ), the distance to the cluster center in units of the core radius  $r_c$ , the countrate with error, and where applicable the identification with sources detected with Einstein (Hertz & Grindlay 1983). The sources are ordered on declination. The positions given are those after correction for bore sight (see text). The positions of the center of the cluster (GC, Djorgovski & Meylan 1993), its core radius and half-mass radius (Trager et al. 1993), and positions of some optical objects discussed in the text are also listed; epochs are 1990.5 for positions by Cool et al., 1979 for USNO-A2, and 1995.5 for HD 116789.

X-ray sources						
X	$\alpha$ (2000)	$\delta$ (2000)	$\Delta$	$d/r_c$	cts/ksec	
4	13 27 27.72	-47 19 8.0	0.4	4.6	$7.8 \pm 0.4$	D
3	13 25 52.05	-47 19 8.6	0.5	5.1	$6.3 \pm 0.3$	A
18	13 26 46.33	-47 19 45.9	1.0	3.4	$0.5 \pm 0.1$	
19	13 27 21.21	-47 23 22.0	1.8	3.1	$0.4 \pm 0.1$	
6	13 27 29.27	-47 25 54.5	1.3	3.0	$0.9 \pm 0.2$	
20	13 26 48.70	-47 27 46.5	1.0	0.4	$0.6 \pm 0.1$	
9a	13 26 53.39	-47 29 1.5	0.9	0.5	$0.9 \pm 0.1$	C
7	13 26 19.75	-47 29 11.9	0.8	1.7	$1.4 \pm 0.2$	B
9b	13 26 52.04	-47 29 37.2	0.9	0.6	$1.1 \pm 0.2$	C
21	13 26 48.99	-47 31 28.1	2.1	1.1	$0.5 \pm 0.1$	
10	13 26 25.20	-47 32 28.9	1.4	2.0	$0.7 \pm 0.1$	
13	13 26 11.12	-47 37 11.1	3.7	4.0	$1.3 \pm 0.3$	
optical objects						
GC	13 26 45.9	-47 28 37			$r_c = 155''$ , $r_h = 288''$	
4	13 27 27.37	-47 19 6.2			Cool et al. (1995a)	
4	13 27 27.68	-47 19 6.3			USNO-A2 0375-18249604	
3	13 25 51.79	-47 19 7.0			Cool et al. (1995a)	
3	13 25 52.23	-47 19 7.5			USNO-A2 0375-18177834	
18	13 26 46.33	-47 19 45.9			HD 116789	
E	13 29 18.54	-47 22 50.5			Margon & Bolte (1987)	

outside the cluster core, and it appears that only source C is clearly related to the globular cluster (e.g. Verbunt et al. 1995). Source E has tentatively been identified with a foreground K star (Margon & Bolte 1987). The sources A and D have been identified with foreground M stars, on the basis of better positions for the X-ray sources obtained with Einstein and ROSAT HRI observations (Cool et al. 1995a). A ROSAT PSPC pointing indicates that source C, near the cluster center, is composed of two sources of comparable luminosity (Johnston et al. 1994).

We have analysed all observations listed in Table 1. The 1992 and 1993 data have been reported on before by

1995. We use this observation as the basis for comparison with the other observations.

### 3.1. Source list and membership probability

In the July 1995 observation we detect twelve sources, listed in Table 2. Eight of these sources have been detected before with Einstein or with the ROSAT PSPC observation reported by Johnston et al. (1994); four sources are new.

The sources X 3 and X 4 are the Einstein sources A and D, respectively, identified with foreground M dwarfs by Cool et al. (1995a, see Table 2). Both stars can be found in the USNO-A2 catalogue (Monet et al. 1998, see Table 2). The new source X 18 can be identified with HD 116789; this is star TYC 8252 4627 1 in the Tycho Reference Catalogue, and thus its position and proper motion are well known (Høg et al. 1998). For this reason we use this star to determine the bore sight correction, i.e. the offset between the X-ray coordinates and the optical coordinates. The result is listed in Table 1.

This bore sight correction has been applied to the X-ray positions, and the resulting positions are given in Table 2. With a statistical accuracy for the X-ray position of X 18 of  $\sim 1''$ , and taking into account small additional systematic errors (see Hasinger et al. 1998), we estimate the systematic error in the positions given in Table 2 to be less than  $2''$ ; for each individual source its statistical uncertainty should be added in quadrature to this systematic error. The positional accuracy can be improved if accurate astrometry of X 3/A and X 4/D is obtained, which will allow computation of their positions at epoch 1995.5.

In the ROSAT Deep Survey (Hasinger et al. 1998), an area with  $12.5$  radius contains 25 sources brighter than our approximate detection limit of  $0.7 \times 10^{-14} \text{ erg cm}^{-2} \text{ s}^{-1}$ ; we thus expect  $\sim 1$  serendipitous source within the core radius, i.e. the faintest source within the core radius, X 20, may well be a serendipitous background source. The brighter sources within the core radius probably are associated with  $\omega$  Cen. Outside the core radius a source is more likely to be a fore- or background source than a cluster member.

### 3.2. Sources in the cluster

The X-ray image of the inner area of  $\omega$  Cen is shown in Fig. 1. The half-mass radius of the cluster contains five sources. Source X 9 from Johnston et al. (1994) is clearly separated into two sources, which we denote X 9a and X 9b for the northern and southern source, respectively.

We have determined the countrates or upper limits for the six central sources in all ROSAT HRI observations of  $\omega$  Cen listed in Table 1. For the very short observations, no

four of the central sources in Fig. 2. We also show the PSPC observation, dividing the PSPC counts for PSPC-X 9 equally between X 9a and X 9b. For the absorption towards  $\omega$  Cen and a black body spectrum of 0.6 keV the PSPC countrate is about 2.8 times the HRI countrate; for smaller reddening the PSPC-to-HRI count ratio varies rapidly, and therefore we do not show PSPC points of the foreground M dwarfs, whose absorption is unknown.

There is marginal evidence for variability in sources X 9b and X 10; and no evidence for variability of X 7 and X 9a. X 20 is detected only in July 1995 and in 1996, X 21 only in July 1995, and all upper limits in the other observations are compatible with the faint fluxes of these sources.

The July 1995 observation was obtained in two parts, separated by about 10 days. We have analysed the two parts separately, and find marginal variation of X 7 ( $1.7 \pm 0.3$  and  $1.1 \pm 0.2$  cts ksec $^{-1}$  in the first and second half, respectively) and of X 9b ( $0.8 \pm 0.2$  and  $1.4 \pm 0.2$  cts ksec $^{-1}$ , respectively). In addition, virtually all counts of X 21 are from the first part of the observation. The number of counts of X 21 is too small for further subdivision.

To convert the observed countrates into X-ray luminosities, we assume a column and distance to  $\omega$  Cen as given in Table 2. For an 0.6 keV blackbody (see the analysis of the PSPC spectrum of X 9 in Johnston et al. 1994) 1 cts ksec $^{-1}$  in the ROSAT HRI corresponds to  $1.5 \times 10^{32} \text{ erg s}^{-1}$  in the 0.5–2.5 keV band. The two sources X 9a and X 9b thus have about this luminosity, source X 7 is 40% brighter, and sources X 20 and X 21 are 40% fainter.

### 3.3. Sources not related to the cluster

The foreground dwarfs (Einstein X-ray sources A and D) are highly variable, as has been pointed out before (Koch-Miramond & Aurière 1987, Cool et al. 1995a). These sources also vary between the first and second half of the July 1995 observation. The extremely high flux of A in 1996 is due to a flare, which lasts almost a day (see Fig. 3).

HD 116789 is an A0V star. From its magnitude  $V = 8.40$  and colour  $B - V = 0.07$  we estimate  $A_V = 0.22$  and a distance of about 310 pc. For an assumed bremsstrahlung spectrum of 1.4 keV the observed countrate corresponds to a luminosity in the 0.5–2.5 keV band of  $\sim 2 \times 10^{29} \text{ erg s}^{-1}$ . It is not expected for an A0V star to emit such a flux; perhaps this star has a white dwarf companion which is responsible for the X-ray emission, as various other A0V stars detected with ROSAT; on the other hand, various apparently single A0V stars in the Bright Star Catalogue have been detected at similar and higher luminosities as HD 116789 (e.g. HD 17864, Hünsch et al. 1998). HD 116789 was detected with EXOSAT by Verbunt et al. (1986), who interpreted the detection as due to the ultraviolet leak of the CMA detector. The EXOSAT CMA

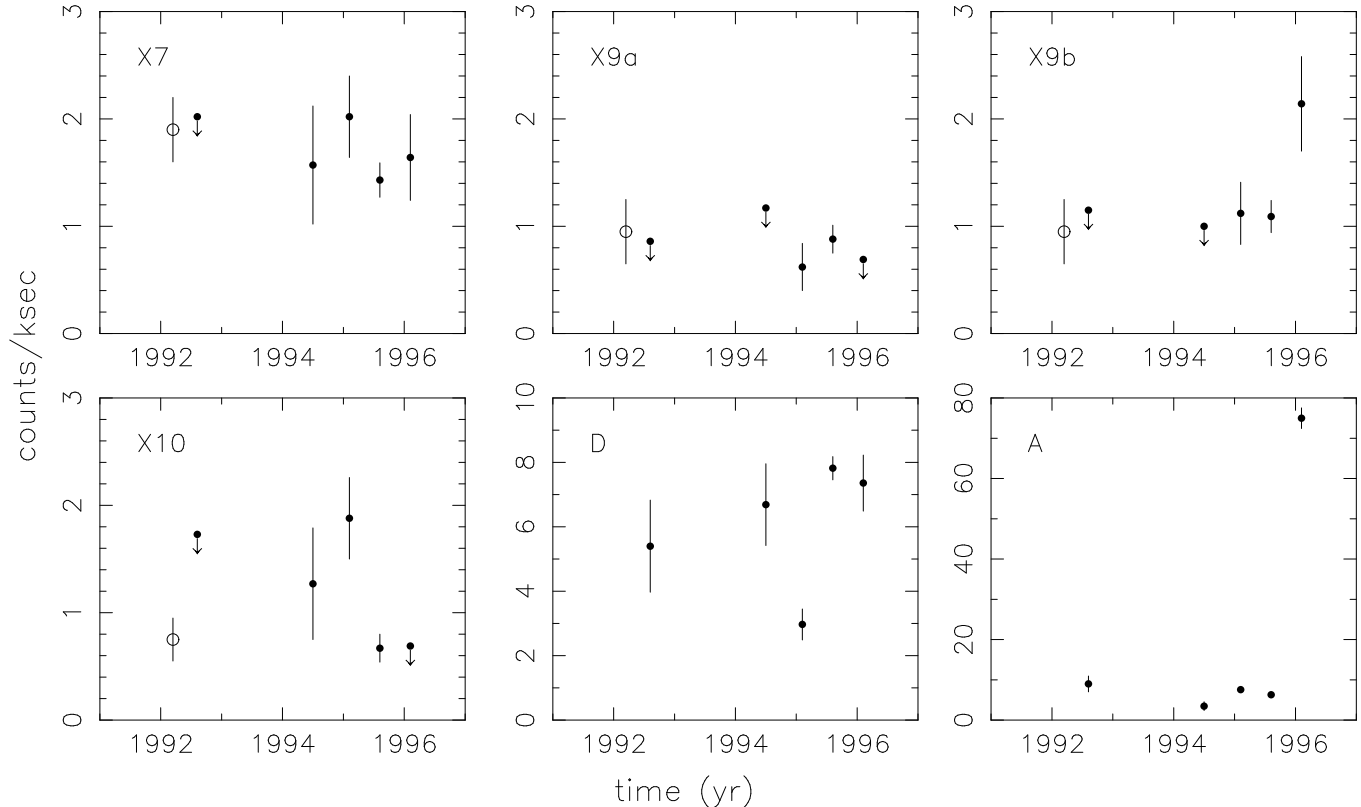


**Fig. 2.** X-ray lightcurves of four sources in the center of  $\omega$  Cen and of two foreground M dwarfs (A, D). The HRI data are shown as  $\bullet$  (detections, with  $1\text{-}\sigma$  errors),  $\downarrow$  ( $2\text{-}\sigma$  upper limits). PSPC data (converted to estimated HRI countrates) are shown as  $\circ$ . There is marginal evidence for variability in sources X9b and X10; the foreground sources A and D are highly variable, with source A showing a large flare in 1996.

$\sim 10^{31}$  ergs $^{-1}$ , much higher than the luminosity derived for this star from the ROSAT observations; we therefore still think that the EXOSAT countrate is due to the ultraviolet flux. The ultraviolet leak in the ROSAT HRI is far too small (Berghöfer et al. 1999) to explain the ROSAT detection.

### 3.4. Discussion

The positions of the sources within the half-mass radius of  $\omega$  Cen as given in Table 2 are more accurate than previously published positions, and may be used to search for optical counterparts. We have done this among the variables (contact binaries, detached binaries, and suspected RS CVn stars) found in  $\omega$  Cen by Kaluzny et al. (1996, 1997): no counterpart is among these stars. (Only one of these variables is in the area shown in Fig. 1, viz. the contact binary OGLEGC 13.) Our non-detection of these binaries is not surprising, considering that our detection limit is above  $10^{31}$  ergs $^{-1}$ : all of the contact binaries hitherto detected in X-rays (McGale et al. 1996), and many

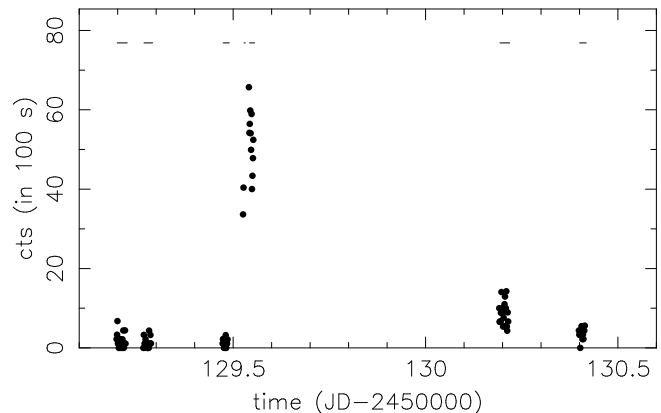


**Fig. 3.** Lightcurve of X3/A in the 1996 observation.  $\bullet$  indicate the numbers of counts collected in 100 s intervals; the horizontal lines indicate when ROSAT was collecting data.

Cool et al. (1995a) argue that X7/B is an extended source. This source is detected in the ROSAT PSPC observation (Johnston et al. 1994) and in the ROSAT HRI

and 1993 observations used by Cool et al. (1995a); in all of them X 7/B is compatible with being a point source.

With the identification of sources X 3 and X 4 with foreground stars, we can reinvestigate the suggested identification of X 5/E with a foreground K star, as suggested by Margon & Bolte (1987). We use the optical positions of A and D to determine the offset between the X-ray positions of the PSPC observation as listed in Johnston et al. (1994) and the optical positions. We then apply this offset to the position of X 5, and find that the resulting position is at  $6 \pm 5$  arcseconds from the optical star. We take the position of the optical star (Table 2) from USNO A2 0375-18334783 (Monet et al. 1998). Identification of X 5 with the foreground star is therefore a distinct possibility.

#### 4. NGC 6397

NGC 6397 is a nearby cluster, with a collapsed core, in or close to which Cool et al. (1993) detected four X-ray sources (B, C1-3) with a ROSAT HRI observation. Photometry with the Hubble Space Telescope enabled Cool et al. (1995b) to find eight candidate counterparts for these sources, on the basis of high ultraviolet flux or of  $H\alpha$  emission. The  $H\alpha$  emission of three stars has been confirmed spectroscopically by Grindlay et al. (1995) who argue that these stars are cataclysmic variables, and responsible for the X-ray emission close to the core.

##### 4.1. Source list and membership

We analyse first the longest observation, obtained in 1995, and use this as a reference for our discussion of the earlier, shorter observations. The standard analysis provides 14 sources, listed in Table 3. Identifications with earlier X-ray sources or optical objects are indicated; 7 sources are new. X 6 has been identified by Cool et al. (1993) as SAO 244944. This star is identical to HD 160177, and is in the Hipparcos Catalogue as HIP 86569. Its position and proper motion are thus very accurately known, and we use it to determine the bore sight correction. This bore sight correction is given in Table 1, and is applied to the X-ray positions; the resulting positions are given in Table 3. The statistical uncertainty in the X-ray position of X 6 is about  $0.5''$ ; we therefore estimate that systematic error of the X-ray positions listed in Table 3 is better than  $1''$ ; this error should be added in quadrature to the statistical error for each individual source position. The quasar identified by Cool et al. (1993) with X 5 coincides within the error with our position for X 5. However, the active galaxy identified by Cool et al. (1993) with X 2 is  $10''$  from our X-ray position, mainly in right ascension; and we conclude that it is not the X-ray source. The explanation probably lies in the new scale for the size of the HRI pixel that we use

**Table 3.** X-ray sources detected in the NGC 6397 ( $A_V = 0.56$ ,  $d = 2.2$  kpc, Djorgovski 1993) with the ROSAT HRI, for the standard analysis of the whole field, and separately for two multi-source analyses of the central area. Numbers up to 10 are sources from Johnston et al. (1994), higher numbers are new; cross-identifications with sources discussed by Cool et al. (1993) are listed on the right. All X-ray positions have been corrected for boresight. The positions of the center of the cluster (GC, Djorgovski & Meylan 1993), its core radius and half-mass radius (Trager et al. 1993) and the positions of some optical objects discussed in the text are also listed; epochs are 1992.7 for positions by Cool et al., and 1996.3 for HIP 86569.

X	$\alpha$ (2000)	$\delta$ (2000)	$\Delta$	$d/r_c$	cts/ksec
X-ray sources in HRI field					
2	17 41 34.79	-53 32 2.0	0.8	230	4.9 $\pm$ 0.3 G
11	17 40 51.16	-53 33 49.0	2.0	135	0.4 $\pm$ 0.1
12	17 40 48.85	-53 39 46.0	1.2	25	0.4 $\pm$ 0.1
13 <sup>a</sup>	17 40 41.56	-53 40 6.0	0.5	6.3	4.6 $\pm$ 0.3 B
4	17 40 42.24	-53 40 23.8	0.4	2.2	7.8 $\pm$ 0.3 C
14	17 40 1.43	-53 42 25.6	1.6	125	0.3 $\pm$ 0.1
15	17 39 16.54	-53 43 11.3	3.7	258	2.8 $\pm$ 0.3
5	17 40 33.18	-53 43 46.6	0.4	72	3.6 $\pm$ 0.2 D
16	17 41 23.73	-53 46 17.2	1.0	172	1.2 $\pm$ 0.2 E
17	17 39 32.92	-53 46 48.7	3.5	240	0.7 $\pm$ 0.2
18	17 40 30.81	-53 47 51.4	0.8	152	1.1 $\pm$ 0.1
6	17 41 27.66	-53 48 10.6	0.5	207	5.5 $\pm$ 0.3 F
19	17 40 14.53	-53 50 31.7	2.8	217	0.6 $\pm$ 0.1
8	17 40 10.46	-53 50 54.7	1.7	229	1.4 $\pm$ 0.2
<sup>a</sup> position affected by nearby source 4					
X-ray sources near center; 5-source fit					
13	17 40 41.44	-53 40 3.3	0.3		3.1 $\pm$ 0.2 B
4a	17 40 42.47	-53 40 28.6	0.5		2.4 $\pm$ 0.3
4b	17 40 42.55	-53 40 19.1	0.5		2.5 $\pm$ 0.2 ID 3
4c	17 40 41.68	-53 40 19.0	0.9		1.2 $\pm$ 0.2 ID 1
4d	17 40 41.64	-53 40 27.7	0.7		1.5 $\pm$ 0.3
X-ray sources near center; 6-source fit <sup>b</sup>					
13	17 40 41.44	-53 40 3.3	0.3		3.1 $\pm$ 0.2 B
4a	17 40 42.24	-53 40 28.6	0.4		1.7 $\pm$ 0.3 ID 2
4b	17 40 42.57	-53 40 19.3			2.6 $\pm$ 0.2 ID 3
4c	17 40 41.52	-53 40 19.4			1.1 $\pm$ 0.2 ID 1
4d	17 40 41.56	-53 40 27.7	0.8		1.2 $\pm$ 0.2
4e	17 40 42.65	-53 40 27.6			1.1 $\pm$ 0.3 ID 6
<sup>b</sup> positions of ID 1, 3 and 6 fixed relative to ID 2					
optical objects					
GC	17 40 41.3	-53 40 25	$r_c = 3''$ , $r_h = 174''$		
5	17 40 33.4	-53 43 45.	D Cool et al. (1993)		
2 <sup>c</sup>	17 41 35.9	-53 32 4.	G Cool et al. (1993)		
6	17 41 28.0	-53 48 13.	F Cool et al. (1993)		
6	17 41 27.66	-53 48 10.6	HIP 86569/HD 160177		
<sup>c</sup> suggested identification probably wrong					

The flux detection limit is about  $0.8 \times 10^{-14}$  erg cm<sup>-2</sup>s<sup>-1</sup> outside the blended central region, similar to that obtained for  $\omega$  Cen. Analogous to

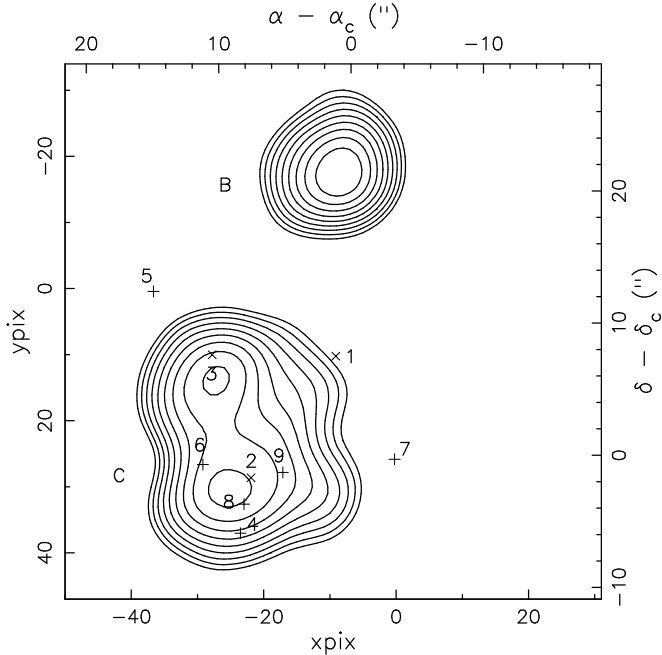


**Fig. 4.** Positions of ultraviolet or  $H\alpha$ -emission objects in the central area of NGC 6397 ( $\times$ ,  $+$ , numbered with their ID in Table 2 of Cool et al. 1995b) superposed on X-ray contours of sources X13/B and X4/C as observed with the ROSAT HRI in 1995. The candidate counterparts for three X-ray sources suggested by Cool et al. are marked  $\times$ . The X-ray image was smoothed with a 2-d  $\sigma \approx 2''$  Gaussian. The lower and left axes give pixel numbers for the ROSAT HRI detector, the upper and right axes right ascension and declination with respect to the cluster center. The conversion between pixel and celestial coordinates is accurate to within  $1''$ .

expect 1.4 background sources within  $3'$  from the center of of NGC 6397; the sources at  $0.5 < r < 3'$  therefore may be background sources. We thus cannot decide whether X12 is a cluster member. Outside the half-mass radius, the sources are more likely to be background or foreground sources. X5, just outside the half-mass radius, is a quasar (Cool et al. 1993).

#### 4.2. The central sources

In Fig.4 we show the X-ray contours of the center of NGC 6397 together with the ultraviolet and/or  $H\alpha$ -emission stars discovered by Cool et al. (1995b). The first models we investigated as fits to the central area of  $60'' \times 60''$ , containing sources X13/B and X4/C, are those with successively one, two, three, four and five sources; all with free positions. Using the  $\Delta L$  criterion for significance (see Sect. 2) we find that five sources are required. We re-

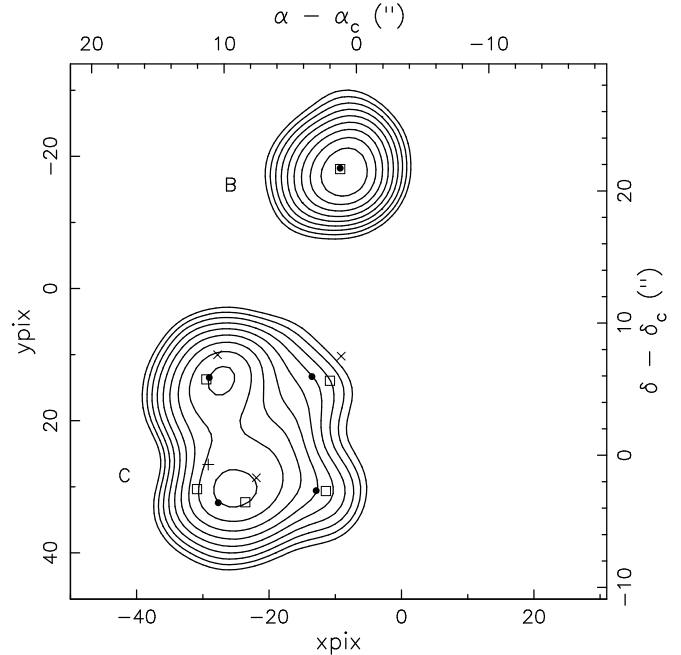


**Fig. 5.** X-ray contours in the central area of NGC 6397 as observed with the ROSAT HRI in 1995, with the positions of the sources obtained in the best fits.  $\bullet$  positions found with the best fit for four components in C in which all positions are left free (Model I),  $\square$  positions found with the best fit for five components in C, in which three sources have distances fixed with respect to one other source, at the distances of ID 1, 3, and 6 to ID 2 (Model IV). Other symbols as in Fig. 4. Model I is marginally better at the 2-sigma level.

do not detect source A of Cool et al. (1993) in the 1995 observation.

Cool et al. (1995b) resolved source X4/C into three components C1-3. From a list of  $H\alpha$  emission and/or ultraviolet excess objects (their Table 2), they suggest identifications of ID 1 with C2, ID 2 for C3 and ID 3 for C1. Comparing the positions of the sources in Model I we find that the positions of X4b and X4c are compatible with those of ID 3 and ID 1, respectively; we thus identify X4b with C1 and X4c with C2. X4d is a new source. (The offset required to match these positions from Table 3 with those given by Cool et al. (1995b) is slightly larger than our claimed accuracy of  $\lesssim 1''$ ; the remaining difference may be explained by an offset between the Guide Star Catalogue coordinate system and the more accurate Hipparcos coordinate system.) The position of X4a is not compatible with that of ID 2. The reason for this may be seen in Fig. 4: the two brightest components of source X4/C have a smaller difference in right ascension than ID 2 and ID 3. If ID 2 is the correct identification for C3, we conclude that X4a is not identical to C3.

**Table 4.** Results of fitting four models to the three data sets of NGC 6397. The Table lists the number  $n$  of fitted parameters, and the difference  $\Delta L$  with respect to the best model for a given data set. In all fits, the fluxes of all sources are fitted parameters. For the 1995 observation Model I has four sources with free positions, Model IV has six sources of which three have free positions and three have fixed positions relative to ID 3, corresponding to the offsets of ID 1, ID 2, and ID 6 with respect to ID 3. Models II and III are as Model IV, after removing ID 6 and ID 2, respectively. For each Model, the same positions as in the best fit for 1995 are used for the 1991 and 1992 data.

Model	1995		1991		1992	
	n	$\Delta L$	n	$\Delta L$	n	$\Delta L$
I (B+4)	16	$\equiv 0$	8	1.3	8	4.7
II (B+1+ID 123)	12	26	8	1.4	8	7.8
III (B+1+ID 136)	12	26	8	3.2	8	$\equiv 0$
IV (B+1+ID 1236)	13	6.2	9	$\equiv 0$	9	1.9

sources must match the distances between the proposed optical counterparts, which are accurately known from the HST observations. In Model II we fit five sources to the X-ray data of the center of NGC 6397, of which three are forced to be at fixed relative positions, corresponding to the distances between ID 1, ID 2 and ID 3. Model II thus has four fitted parameters less than Model I. The  $\ln L$  of Model II is 26 higher than that of Model I, i.e. it is a significantly (4-sigma) worse fit. This confirms that X 4a is not ID 2. In Model III we assume that ID 6 of Table 2 in Cool et al. (1995b) rather than ID 2 is the counterpart of C3, and fix the distances between the sources accordingly. This fit has the same  $\ln L$  as Model II, and thus also is significantly worse than the fit of Model I. Again, the reason for the bad fit is the mismatch in the difference in right ascensions of the two brightest X-ray sources with that between the proposed counterparts: X 4a is not ID 6.

We note that the best position of X 4a is between ID 2 and ID 6, and in Model IV we fit six sources, of which four are forced to be at the relative distances of ID 1-3 and ID 6. Model IV thus has three fitted parameters less than Model I. Its  $\ln L$  is 6 higher than that of Model I, i.e. it is marginally worse at less than 2-sigma. The parameters of the six sources of this model are also given in Table 3. It is seen that the positions of X 4b, X 4c and X 4d are the same (within the error) in Model IV as in Model I.

Thus, we have two acceptable models. In both models we confirm the possible identifications of ID 3 with C1 (=X 4b) and of ID 1 with C2 (=X 4c), and we find one new source (X 4d). In Model I the remaining flux is ascribed to one source (X 4a) which is not identical to ID 2. In Model IV the remaining flux is ascribed to two sources, one of which is ID 2/C3 and one is a second new source,

**Table 5.** Countrates (counts  $\text{ksec}^{-1}$ ) assigned to the central sources in Models I and IV in the fits to the observations of 1991 and 1992. Numbers in parentheses indicate the errors in the last digit. For 1995 see Table 3.

X	Model I		Model IV	
	1991	1992	1991	1992
13	2.3(7)	2.9(5)	13	2.5(7) 2.8(6)
4a	1.4(6)	0.8(4)	4a	1.5(8) 0.7(5)
4b	2.2(7)	2.1(5)	4b	2.2(7) 2.1(6)
4c	1.8(7)	2.5(5)	4c	1.9(7) 2.3(6)
4d	0.9(6)	0.9(4)	4d	0.7(6) 0.8(4)
			4e	< 0.6 0.4(3)

#### 4.3. The earlier observations

The standard analysis detects X 2, X 5, X 16, X 6 and X 8 in both the 1991 and the 1992 data of NGC 6397, and X 19 in the 1992 data, all at countrates compatible with those of 1995. It also detects sources X 13/B and X 4/C in the 1991 data and in the 1992 data, labelling both as extended. The number of photons in sources B and C is rather small in these short observations. To limit the number of parameters in the fits to the central sources we demand that the distance between the fitted central sources in each model is the same as in the best fit to the 1995 data, but allow the fluxes to be different. The corresponding reductions in the number of fitted parameters for each model are indicated in Table 4.

We thus fit four models to each data set. For each year, the best model is set at  $\Delta L \equiv 0$ , and the quality of the other models for that year is determined with respect to this model. The results of our fitting are shown in Table 4. For the 1991 data, the models with five sources are comparable in quality, and the six-source model is not significantly better. For the 1992 data, Model III is marginally better (2 sigma) than Model I and significantly (3 sigma) better than Model II, whereas Model IV is of similar quality.

The fits to the earlier data confirm the conclusions that we draw on the basis of the observation of the long observation of 1995. Model I in which source X 4/C is separated into four components at free positions is acceptable for all three observations. Model II in which X 4/C is separated into four components at fixed relative distances of ID 1-3, is not acceptable for the 1992 data. Model IV in which X 4/C is separated into five components, four of which correspond to ID 1, ID 2, ID 3 and ID 6, also is acceptable for all observations. ID 2 is not required in 1992, and ID 6 is not required in 1991. The latter fact explains why ID 6 is not present in the analysis by Cool et al. (1993) of the 1991 data. These conclusions are confirmed by the countrates that Model IV ascribes to the different sources, listed in Table 5



1992 observation (after shifting the 1992 observation by  $3''.5, 1''.0$  in  $\alpha, \delta$ ; compatible with the shift as determined by Cool et al.). We fit Model I to the added image, and compare it with the fit in which a source is added to model A. We find  $\Delta L = 10$ , which implies that source A is marginally significant at  $\sim 2.5\sigma$ . The position ( $+2''.4, -14''$  with respect to source B) and countrate (0.4 counts/ks) that we find for source A are compatible with those given by Cool et al. (1993).

#### 4.4. Sources not related to the cluster

HIP 86569 is a K1 IV/V star with  $V = 9.44$ ,  $B - V = 0.90$ , and a parallax of  $0.0167(18)''$ . Hipparcos discovered that this star is a close binary (separation  $0.19''$ ) of stars with Hipparcos magnitudes  $H = 10.17(9)$  and  $10.47(11)$ , respectively. At a distance of 60 pc the observed ROSAT HRI countrate converts to an X-ray luminosity in the 0.5-2.5 keV band of  $L_x \simeq 4 \times 10^{28} \text{ erg s}^{-1}$  (for assumed 1.4 keV bremsstrahlung with no absorption). This is similar to the X-ray luminosities of single KV stars detected in the ROSAT All Sky Survey, such as HD 17925 (K1V) which has  $L_x \simeq 1.2 \times 10^{29} \text{ erg s}^{-1}$  (Hünsch et al. 1998).

#### 4.5. Discussion

The core of NGC 6397 contains at least four X-ray sources detected with ROSAT, and possibly five.  $1 \text{ cts ksec}^{-1}$  for a source at the distance and with the absorption column of NGC 6397, for an assumed 0.6 keV bremsstrahlung spectrum corresponds to a luminosity in the 0.5-2.5 keV band of  $2.2 \times 10^{31} \text{ erg s}^{-1}$ . The faintest source we detect, X 4c, is at this level. The brightest source is X 13/B, at a luminosity of about  $6.8 \times 10^{31} \text{ erg s}^{-1}$ . These luminosities are at the bright end of the luminosity distribution for cataclysmic variables, such as the large sample investigated with ROSAT (Verbunt et al. 1997), as expected for an X-ray selected sample.

Of these sources, X 13 and X 4b have the same flux level in all three observations. Source X 4c is fainter in 1995. The identifications of X 4b and X 4c with cataclysmic variables ID 3 and ID 1 remains probable, as does the argument by Edmonds et al. (1999) that these systems are DQ Her type systems. The distance between X 4b and X 4c in Model I is marginally less than the distance between the proposed counterparts; it is tempting to speculate that this is due to a small X-ray flux contribution of a fourth cataclysmic variable ('CV 4') identified by Cool et al. (1998) and confirmed by Edmonds et al. (1999).

The new source X 4d has been detected in the 1995 observation because of the longer exposure; it may, but need not, be brighter in the 1995 observation than in 1991 and 1992.

If the remaining flux is assigned to one source X 4a,

two sources X 4a and X 4e, the flux of X 4a may still be constant, and X 4a may be identified with the probably DQ Her type cataclysmic variable ID 2. In this case, the flux of X 4e has increased between 1991 and 1995. ID 6 was reported to vary by 1.1 magnitude in five hours by De Marchi & Paresce (1994), but was constant in a ten hour observation by Cool et al. (1998). It is suggested by Edmonds et al. (1999) that ID 6 is a undermassive helium white dwarf, probably in a binary. If it is a single helium white dwarf, it cannot be a variable X-ray source; if it is in a binary with a recycled radio pulsar, it also is unlikely to be a variable X-ray source; if it is in a binary with another white dwarf, then optical and X-ray variability can be due to variable mass transfer from that other white dwarf. However, it is also possible that not ID 6, but a nearby hitherto unidentified star in NGC 6397 is the X-ray source X 4e.

Whether source X 4a alone, or source X 4a and X 4e are present in the core of NGC 6397, and in the latter case whether X 4e is identical to ID 6 requires a better spatial resolution for the X-ray observations than provided by ROSAT.

## 5. NGC 6752

Two sources have been detected in the core and two near the core of NGC 6752 in a ROSAT HRI observation obtained in 1992 (Grindlay 1993); close to one of the core sources, two candidate cataclysmic variables have been identified on the basis of  $H\alpha$  emission and variability on (presumably orbital) periods of 5.1 and 3.7 hrs (Bailyn et al. 1996).

#### 5.1. Data analysis and source list

Two more observations of NGC 6752 have been obtained by us. Because the three observations have comparable length, we add them into a combined image which we analyse and use as a reference for the individual observations. To add the three observations we use the method outlined by Verbunt & Hasinger (1998), as follows. First we correct the data for each observation separately for the changed pixel size (see Sect. 2), analyse the resulting images and determine the offsets between sources detected in separate observations. Averaging these offsets we find (on the basis of sources X 3, X 13, X 4, and X 6) that the X-ray coordinates of the 1996 observation have to be shifted by  $d\alpha = -0''.7 \pm 0''.7$  in right ascension and  $d\delta = +3''.6 \pm 0''.7$  in declination to be brought in line with the 1992 data. Similarly, the 1995 data (on the basis of the same sources plus X 14) must be shifted by  $d\alpha = +2''.4 \pm 0''.7$ ,  $d\delta = +1''.2 \pm 0''.7$ . We apply these corrections to the pixel coordinates of the photons, and then add the three images into a combined image, which is anal-

**Table 6.** X-ray sources detected in NGC 6752 ( $A_V = 0.12$ ,  $d = 4.2$  kpc, Djorgovski 1993) with the ROSAT HRI, for the standard analysis of the whole field, and separately for the multi-source analysis of the central area. Numbers up to 15 are sources from Johnston et al. (1994), higher numbers are new. All X-ray positions have been corrected for boresight. Identifications with letter on the right refer to Grindlay (1993). The positions of the center of the cluster (GC, Djorgovski & Meylan 1993), its core radius and half-mass radius (Trager et al. 1993) and the positions of some optical objects discussed in the text are also listed.

X	$\alpha$ (2000)	$\delta$ (2000)	$\Delta$	$d/r_c$	cts/ksec
X-ray sources in HRI field					
3	19 12 27.01	-59 48 20.1	2.9	87	$3.5 \pm 0.4$
13	19 9 59.88	-59 54 50.6	1.1	42	$1.0 \pm 0.2$
4	19 10 3.26	-59 55 33.9	0.5	38	$3.1 \pm 0.2$
6	19 10 40.23	-59 58 39.3	0.9	8.4	$1.0 \pm 0.1$ A
7	19 10 51.35	-59 59 3.0	0.6	1.0	$3.6 \pm 0.3$ BC
14	19 10 55.73	-59 59 35.9	1.1	4.4	$0.7 \pm 0.1$ D
15	19 10 4.25	-60 2 54.3	0.7	73	$1.8 \pm 0.2$
16	19 10 4.56	-60 3 16.2	0.8	70	$1.5 \pm 0.2$
17	19 11 20.33	-60 3 18.5	1.2	70	$0.5 \pm 0.1$
18	19 10 32.92	-60 3 59.8	1.3	67	$0.5 \pm 0.1$
19	19 11 41.66	-60 5 9.2	2.2	75	$0.6 \pm 0.1$
20	19 10 12.07	-60 6 6.6	1.8	67	$0.6 \pm 0.1$
11 <sup>a</sup>	19 10 57.91	-60 16 16.5	0.9	62	$26.1 \pm 0.7$
<sup>a</sup> position affected by nearby detector edge					
X-ray sources near center					
7a	19 10 51.43	-59 58 56.6	0.5		$1.6 \pm 0.2$ C
7b	19 10 51.20	-59 59 8.2	0.6		$1.7 \pm 0.2$ B
21	19 10 52.51	-59 59 1.9	1.1		$0.5 \pm 0.1$
22	19 10 51.34	-59 59 24.0	1.5		$0.4 \pm 0.1$
optical objects					
GC	19 10 51.8	-59 58 55.		$r_c = 11''$ , $r_h = 115''$	
19	19 11 41.66	-60 05 9.2		TYC 9071 228 1	
11	19 10 57.84	-60 16 19.1		HIP 94235/HD 178085	
16	19 10 04.51	-60 03 18.4		USNO-A2 0225-29896802	
	19 10 51.27	-59 58 53		# 1 Bailyn e.a. 1996	
	19 10 51.18	-59 58 49		# 2 Bailyn e.a. 1996	

We identify two sources with stars with accurate positions: X 19 is close to TYC 9071 228 1 (CD-60 7128), a star with  $V = 9.99$  and  $B = 10.48$ , and X 11 is close to HIP 94235/HD 178085, a G0V star with  $V = 8.38$  and  $B = 9.00$ . The latter identification was suggested already by Johnston et al. (1994) on the basis of the PSPC observation. The chance probability of finding a counterpart at these optical brightnesses is small, and we consider both identifications secure. The X-ray position of X 11 is affected by its proximity to the edge of the HRI detector. For this reason we use X 19 to tie the X-ray to the optical coordinates. X 19 is not found in any of the three individual observations, showing up only in the combined frame. It is a relatively weak source and its position accordingly has an error of  $1''.5$  both in right ascension and in declina-

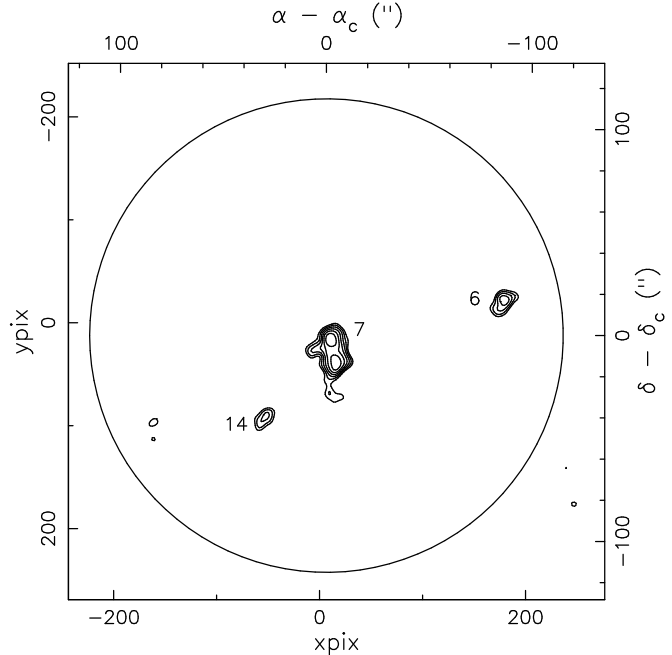


**Fig. 6.** X-ray contours in the central area of NGC 6752 as observed with the ROSAT HRI in the combined image of the 1992-1996 data. The image was smoothed with a 2-d  $\sigma \approx 3''$  Gaussian. The detected sources are indicated with their numbers in Table 2. The circle gives the half-mass radius of the cluster. The lower and left axes give pixel numbers for the ROSAT HRI detector, the upper and right axes right ascension and declination with respect to the cluster center.

to all positions of the X-ray sources; the resulting positions are listed in Table 6. (The remaining offset between X 11 and HIP 94235 is within the nominal error for the right ascension, and within 2-sigma for the declination: note that the error is composed of the statistical uncertainties in the positions of both X 19 and X 11.)

The detection limit in the total observation is about  $0.7 \times 10^{-14}$  erg cm $^{-2}$  s $^{-1}$ . An area with radius  $12.5'$  in the ROSAT Deep Survey contains 25 sources brighter than this limit; we thus expect to find 0.6 in the region within the half-mass radius of NGC 6752,  $r_h \simeq 2'$ . The sources in the core thus probably belong to the cluster, and possibly the two sources X 6/A and X 14/D as well.

### 5.2. Sources in the center of the cluster

Analysing the central source with the method described in Sect. 2, we find four significant sources (the increase in  $\ln L$  is 29 both for the third and for the fourth source). This adds two sources to the two already described by Grindlay (1993). The position and fluxes of these sources are listed in Table 6; Fig. 7 shows the positions and X-

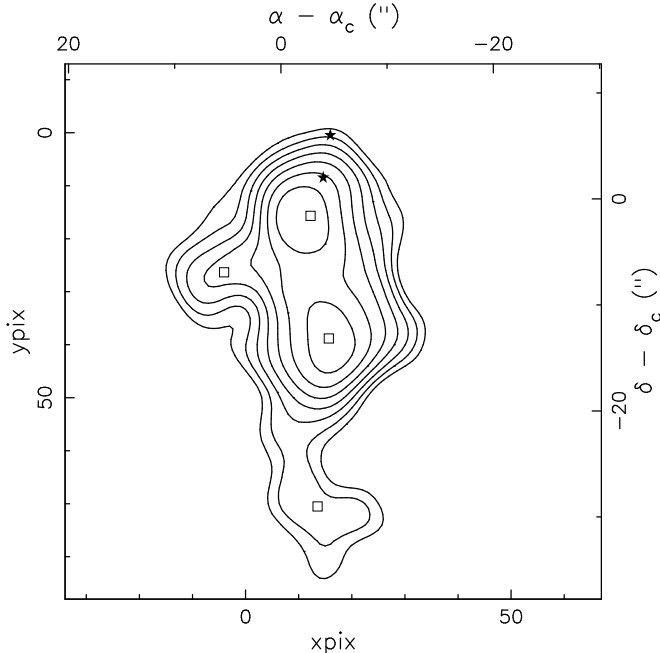


**Fig. 7.** X-ray contours in the central area of NGC 6752 as observed with the ROSAT HRI in the combined data of 1992-1996, with the positions of the sources obtained with the multi-source fit ( $\square$ ). The positions of two candidate cataclysmic variables found by Bailyn et al. (1996) are indicated with  $\star$ .

by Bailyn et al. (1996). The southern cataclysmic variable ('star 1') is at  $3.8 \pm 2.3''$  from X 7a, and therefore remains a possible counterpart (assuming an error of  $1''$  for the optical position, and taking into account the  $2''$  error of X 19).

We have analysed the separate observations, keeping the position of the four central sources fixed at those of the co-added image (as listed in Table 6), but allowing their fluxes to vary. We do not find significant evidence for variation; due to the limited statistics we cannot exclude variations by a factor two.

A countrate of  $1 \text{ cts ksec}^{-1}$  corresponds to a luminosity between 0.5 and 2.5 keV of  $4.6 \times 10^{31} \text{ ergs}^{-1}$  at the distance of NGC 6752 and for an assumed 0.6 keV bremsstrahlung spectrum. Thus, X 7a and X 7b have X-ray luminosities of about  $7.5 \times 10^{31} \text{ ergs}^{-1}$ , and X 21 and X 22 about a quarter of this. X 6 and X 14, the two sources outside the cluster core have luminosities of  $4.6 \times 10^{31} \text{ ergs}^{-1}$  and  $3.2 \times 10^{31} \text{ ergs}^{-1}$ , respectively, if they are in NGC 6752.

### 5.3. Sources not related to the cluster

The spectral type of TYC 9071 228 1 is not known; on the basis of its magnitude and colour ( $V = 9.99$ ,  $B - V =$

$1.4 \text{ keV}$  bremsstrahlung spectrum, the countrate of X 19 converts to an X-ray luminosity in the 0.5-2.5 keV band of  $\sim 3 \times 10^{28} \text{ ergs}^{-1}$ , a reasonable value for a late F main-sequence star (see e.g. the list of ROSAT detections of bright stars by Hünsch et al. 1998). The Tycho Catalogue marks this star with 'unresolved duplicity', with visual magnitude varying between 9.51 and 10.88.

HIP 94235 has a significant parallax which puts it at 57 pc. Its countrate converts to an X-ray luminosity at that distance of about  $2 \times 10^{29} \text{ ergs}^{-1}$ , a normal X-ray luminosity for a G0V star.

Comparison of the ROSAT image with the USNO-A2 Catalogue gives a candidate identification for X 16, at a distance of  $2''.2$ , see Table 6. No other sources outside the cluster have been identified by us.

We have analysed the three separate HRI observations, and find no evidence for variability, except for X 15, which in March 1992 had an X-ray flux about half of that observed in March 1995 and April 1996.

## 6. Liller 1

The globular cluster Liller 1 is a highly reddened cluster near the galactic center ( $A_V \simeq 9.5$ ,  $d = 8.6 \text{ kpc}$ , Frogel et al. 1995). It probably has undergone core collapse (Djorgovski 1993). Liller 1 harbours the Rapid Burster, a highly unusual recurrent transient. When discovered in 1977 the source emitted short ( $\lesssim 5 \text{ s}$ ) bursts of X-rays every  $\sim 10 \text{ s}$ ; in some later observations, e.g. Aug 1985, it emitted bursts of  $\sim 500 \text{ s}$  separated by 1500-4000s; and it has also been observed as a steady source. The bursts are interpreted as accretion events. In addition to these, thermonuclear bursts have also been detected, identifying the accreting star as a neutron star. A review of this remarkable source is given by Lewin et al. (1995). A low-luminosity X-ray source near Liller 1 is tentatively identified as the quiescent (low-state) counterpart of the Rapid Burster (Asai et al. 1996).

No source is detected in the cluster in our ROSAT HRI observation of the globular cluster Liller 1. Near the cluster center, no circle with radius of  $5''$  contains more than 4 photons. For an expected number of 10 photons, the probability of getting 4 or fewer photons is less than 4%. We thus take 10 as the  $2\text{-}\sigma$  upper limit to the number of photons, which with the effective exposure time is converted to an upper limit of  $0.6 \text{ cts ksec}^{-1}$ .

Asai et al. (1996) report the detection on 1993 Aug 27 with ASCA of a source near Liller 1. For a powerlaw with photon index 2, absorbed by a column  $N_H = 10^{22} \text{ cm}^{-2}$ , this source has an unabsorbed flux in the 2-10 keV band of  $2.5_{-0.8}^{+1.7} \times 10^{-13} \text{ erg cm}^{-2} \text{ s}^{-1}$ . For this spectrum our upper limit in the ROSAT HRI corresponds to a flux of  $1.4 \times 10^{-13} \text{ erg cm}^{-2} \text{ s}^{-1}$ , slightly lower than the ASCA detection.

**Table 7.** Positions of the center of Liller 1 (GC, Picard & Johnston 1995) its core radius (Trager et al. 1993) and the positions of X-ray sources detected near it, viz. the Rapid Burster (RB, Hertz & Grindlay 1983), a dim source detected with ASCA (A, Asai et al. 1996) and a dim source detected with the ROSAT HRI (R, this paper). The position of the O star HD 317889 is also given. The final columns gives the errors in the positions.

	$\alpha$ (2000)	$\delta$ (2000)	$\delta\alpha$ (")	$\delta\delta$ (")
GC	17 33 24.5	-33 23 20.4	$r_c = 4''$	
RB	17 33 24.0	-33 23 16.2	2	2
A	17 33 19.0	-33 23	90	30
A <sup>a</sup>	17 33 24.2	-33 23 6.5	20	20
R	17 33 4.76	-33 23 27.2	5	5
HD	17 33 5.02	-33 23 28.4		

<sup>a</sup>new determination by Asai, 1999, private communication

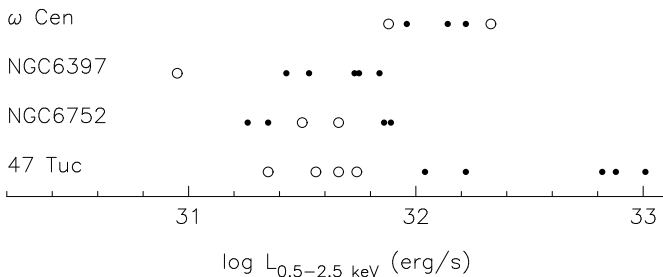


**Fig. 8.** X-ray luminosities of dim sources in four globular clusters. Sources in and outside the core are shown as ● and ○, respectively. Data points are from Table 8, and for 47 Tuc from Verbunt & Hasinger (1998) slightly modified for an assumed 0.6 keV bremsstrahlung spectrum. In all cases the detection limits in and outside the core are close to the lowest detected luminosities in and outside the cores.

error in the position of this source is about  $1''$ ; the actual error is dominated by the error in the bore sight correction, which is about  $5''$ . The ROSAT source is not compatible with the center of Liller 1, and also not compatible with the position of the Rapid Burster as determined with Einstein (see Table 7). The position of the ROSAT source coincides within the bore sight uncertainty with the O4 III(f) star HD 317889 (Vijapurkar & Drilling 1993). The star is in the Tycho Catalogue as TYC 7380 976 1. From the observed magnitude and colours ( $V = 10.12$ ,  $B - V = 0.92$ ,  $U - B = -0.23$ , Drilling 1991) we estimate a reddening and distance of  $E(B - V) \simeq 1.2$  and  $d \simeq 3$  kpc for HD 317889. The observed ROSAT HRI countrate is as expected for such a star, according to the general correlation between bolometric luminosity and X-ray luminosity of O stars:  $L_x \simeq 10^{-7} L_b$  (e.g. Kudritzki et al. 1996). (HD 317888 is within  $1''$  of the O4 star; we have not been able to find more information on this star.)

did detect the Rapid Burster in quiescence, or another low-luminosity source in Liller 1; and that ROSAT observed when this source had a lower flux level. In fact, variation of transients in their quiescent state is common (e.g. Campana et al. 1997). The star detected with ROSAT in this case is not detected with ASCA, presumably because its spectrum is too soft. The second interpretation is that ASCA in fact detected the star also detected with ROSAT, and not the quiescent counterpart of the Rapid Burster. The position of the ROSAT source is marginally compatible with that of the ASCA source; its countrate is exactly that predicted on the basis of the ASCA source. Dr. Asai has kindly communicated a new determination of the position of the X-ray source detected by ASCA, using new calibrations to improve the accuracy. This position, listed in Table 7, excludes the ROSAT source as a possible counterpart, and thus confirms that ASCA indeed detected a source in the cluster.

## 7. Summary and discussion

In the three low-reddened clusters  $\omega$  Cen, NGC 6397 and NGC 6752 we have detected a total of 17 dim X-ray sources, of which 5 are well outside the core. The X-ray luminosities of these sources are listed in Table 8, and plotted in Fig. 8. The interpretation of Fig. 8 must be made with some care. First, sources outside the core may not belong to the cluster; the faintest core source in  $\omega$  Cen may be a fore- or background source. Second, the conversion of observed countrate to luminosity depends on the assumed spectrum, and from PSPC observations we know that different sources have different spectral parameters (Johnston et al. 1994). For example, the 0.6 keV black body spectrum used for the sources in  $\omega$  Cen gives a 40% higher flux for the same countrate than an assumed 0.6 keV bremsstrahlung spectrum would give. The bremsstrahlung spectrum is used for the three other clusters. Third, the detection limits in NGC 6397, NGC 6752 and 47 Tuc are higher in the cores, where the point spread functions of sources overlap, than outside the core. Such a difference is not present in  $\omega$  Cen. Fourth, we show the average luminosity, and several sources are known to be variable.

With these points in mind, we note from Fig. 8 that in all clusters except possibly  $\omega$  Cen the most luminous sources appear to be in the cluster core. The main difference between  $\omega$  Cen and the other clusters is that the collision frequency in  $\omega$  Cen is so low that one expects no low-mass X-ray binaries in it, and that most cataclysmic variables in it will be evolved from primordial binaries (Verbunt & Meylan 1988, Davies 1997). In addition, the mass segregation in this cluster is very low. Thus in  $\omega$  Cen there is no marked difference between the core and the regions outside the core.

**Table 8.** X-ray luminosities in  $\text{erg s}^{-1}$  in the 0.5-2.5 keV band of the dim X-ray sources in globular clusters described in this paper. For sources in  $\omega$  Cen we assume a 0.6 keV black body spectrum; for those in NGC 6397 and NGC 6752 a 0.6 keV bremsstrahlung spectrum. For the same countrate, the blackbody spectrum corresponds to a flux higher by about 40% than the bremsstrahlung spectrum.

$\omega$ Cen		NGC 6397		NGC 6752	
X	$\log L_x$	X	$\log L_x$	X	$\log L_x$
core		core		core	
9a	32.14	13	31.84	7a	31.86
9b	32.22	4a	31.73	7b	31.89
20	31.96	4b	31.75	21	31.35
	outside	4c	31.43	22	31.26
7	32.33	4d	31.53		outside
21	31.88		outside	6	31.66
		12	30.95	14	31.50

will detect more sources. In the cores of NGC 6397 and NGC 6752 the detection of more source will also require better imaging, so that the faint sources can be detected against the brighter ones. We do not detect a difference between the luminosities of sources in the collapsed globular cluster NGC 6397 and the much less concentrated globular cluster NGC 6752. On the other hand, the highly concentrated cluster 47 Tuc contains three sources which are an order of magnitude brighter than the brightest sources in NGC 6397 and NGC 6752.

Viable optical counterparts have been suggested for only five among the 26 sources shown in Fig. 8, all of them probable cataclysmic variables. We compare the ratio of X-ray flux to optical flux of these sources with the ratios measured for cataclysmic variables and for RS CVn systems in the Galactic Disk in Fig. 9. It is seen that the suggested optical counterparts for the sources in NGC 6397 and NGC 6752 lead to ratios which are compatible with those of cataclysmic variables, whereas those in 47 Tuc are too bright in X-rays, in agreement with Fig. 8. If these sources are indeed cataclysmic variables, their excessive X-ray luminosity needs to be explained; alternatively, the suggested identifications may be chance coincidences (as discussed by Verbunt & Hasinger 1998). All suggested counterparts lead to higher X-ray to optical flux ratios than those of RS CVn binaries.

The accurate positions that we determine for individual sources are valid for separately detected sources in particular. In the case of overlapping sources, we do not have unique solutions. Thus, in the core of NGC 6397 fits with 5 and 6 sources are both acceptable, at similar quality; and we cannot exclude that more sources contribute to the observed flux, which would invalidate our derived positions.

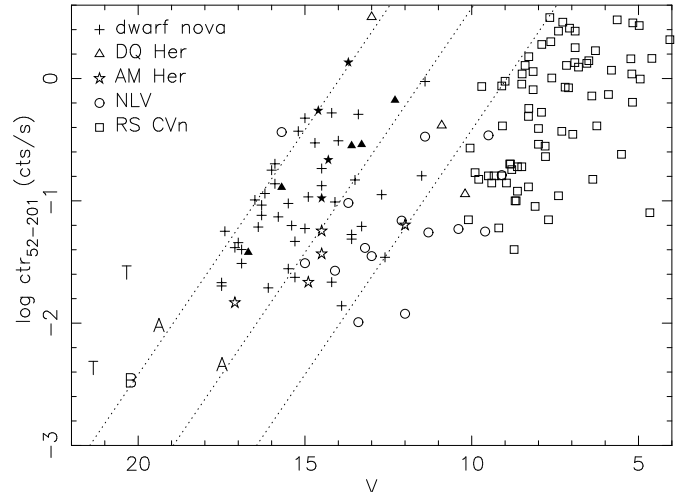


**Fig. 9.** X-ray countrates of the dim sources in globular clusters as a function of their visual magnitude, compared with the ROSAT PSPC countrates and visual magnitudes of various types of cataclysmic variables (data from Verbunt et al. 1997; filled symbols represent systems first discovered in X-rays and only subsequently identified as cataclysmic variables, i.e. X-ray selected systems) and with RS CVn systems (data from Dempsey et al. 1993) respectively. PSPC countrates of the dim cluster sources have been computed for an assumed 0.6 keV bremsstrahlung spectrum, corrected for absorption, from the observed HRI countrates. Visual magnitudes are also corrected for absorption. T indicate sources in 47 Tuc (X 9 and X 19,  $V$  as estimated by Verbunt & Hasinger 1998), A in NGC 6397 (X 4b and X 4c,  $V$  from Cool et al. 1998), B in NGC 6752 (X 7a,  $V$  from Bailyn et al. 1996). The dotted lines indicate a constant ratio of X-ray to optical flux.

cause a three-body interaction (i.e. a close encounter of a binary with a single star) in the core has expelled the binary from the core (e.g. Hut et al. 1992). In the latter case the binary is expected to be eccentric immediately after being expelled; tidal forces may in time circularize the orbit again. Such binaries are only a minority of the overall binary population of a cluster; however, X-ray observations may preferably select such binaries if tidal forces act in them. Since sources away from the core can be foreground or background sources, optical identification of them is required to settle whether they belong to the cluster or not. Our accurate positions should help in finding such counterparts.

*Acknowledgements.* We have made use of the ROSAT Data Archive of the Max Planck Institut für extraterrestrische Physik at Garching; of the SIMBAD database operated at Centre de Données astronomiques in Strasbourg; and of the Digitized Sky Surveys. For Hipparcos and Tycho data the CD-ROM Celestia, provided by ESA, was very helpful. We further

the Digitized Sky Surveys, and Dr. Asai for communication of the re-determination of the position of the ASCA source in Liller 1.

## References

- Asai, K., Dotani, T., Kunieda, H., Kawai, N. 1996, *Publ. Astr. Soc. Japan*, 48, L27
- Bailyn, C., Rubenstein, E., Slavin, S., et al. 1996, *ApJ (Letters)*, 473, L31
- Berghöfer, T., Schmitt, J., Hünsch, M. 1999, *A&A*, 342, L17
- Campana, S., Mereghetti, S., Stella, L., Colpi, M. 1997, *A&A*, 324, 941
- Cash, W. 1979, *ApJ*, 228, 939
- Cool, A., Grindlay, J., Bailyn, C., Callanan, P., Hertz, P. 1995a, *ApJ*, 438, 719
- Cool, A., Grindlay, J., Cohn, H., Lugger, P., Bailyn, C. 1998, *ApJ (Letters)*, 508, L75
- Cool, A., Grindlay, J., Cohn, H., Lugger, P., Slavin, S. 1995b, *ApJ*, 439, 695
- Cool, A., Grindlay, J., Krockenberger, M., Bailyn, C. 1993, *ApJ (Letters)*, 410, L103
- Cruddace, R., Hasinger, G., Schmitt, J. 1988, in F. Murtagh, A. Heck (eds.), *Astronomy from large databases*, p. 177
- Danner, R., Kulkarni, S., Thorsett, S. 1994, *ApJ (Letters)*, 436, L153
- David, L., Harnden, Jr, F., Kearns, K., Zombeck, M. 1995, *The ROSAT High Resolution Imager (HRI)*, Technical report, U.S. ROSAT Science Data Center/SAO
- Davies, M. 1997, *MNRAS*, 288, 117
- de Marchi, G., Paresce, F. 1994, *A&A*, 281, L13
- Dempsey, R., Linsky, J., Fleming, T., Schmitt, J. 1993, *ApJS*, 86, 599
- Djorgovski, S. 1993, in S. Djorgovski, G. Meylan (eds.), *Structure and Dynamics of Globular Clusters*, Vol. 50 of *ASP Conference Series*, ASP, p. 373
- Djorgovski, S., Meylan, G. 1993, in S. Djorgovski, G. Meylan (eds.), *Structure and Dynamics of Globular Clusters*, Vol. 50 of *ASP Conference Series*, ASP, p. 325
- Drilling, J. 1991, *ApJS*, 76, 1033
- Edmonds, P., Grindlay, J., Cool, A., et al. 1999, *ApJ*, 516, 250
- ESA 1997, *The Hipparcos and Tycho Catalogues*, ESA SP 1200
- Frogel, J., Kuchinski, L., Tiede, G. 1995, *AJ*, 109, 1154
- Grindlay, J. 1993, in S. Djorgovski, G. Meylan (eds.), *Structure and Dynamics of Globular Clusters*, Vol. 50 of *ASP Conference Series*, ASP, p. 285
- Grindlay, J., Cool, A., Callanan, P., et al. 1995, *ApJ*, 455, L47
- Hakala, P., Charles, P., Johnston, H., Verbunt, F. 1997, *MNRAS*, 285, 693
- Hasinger, G., Burg, R., Giacconi, R., et al. 1998, *A&A*, 329, 482
- Hertz, P., Grindlay, J. 1983, *ApJ*, 275, 105
- Høg, E., Bässgen, G., Bastian, U., et al. 1997, *A&A*, 323, L57
- Høg, E., Kuzmin, A., Bastian, U., et al. 1998, *A&A*, 335, L65
- Hünsch, M., Schmitt, J., Voges, W. 1998, *A&AS*, 132, 155
- Johnston, H., Verbunt, F. 1996, *A&A*, 312, 80
- Johnston, H., Verbunt, F., Hasinger, G. 1994, *A&A*, 289, 763
- Kaluzny, J., Kubiak, M., Szymanski, M., et al. 1997, *A&AS*, 122, 471
- Koch-Miramond, L., Aurière, M. 1987, *A&A*, 183, 1
- Kudritzki, R. P., Palsa, R., Feldmeier, A., Puls, J., Pauldrach, A. W. A. 1996, in H. Zimmermann, J. Trümper, H. Yorke (eds.), *Roentgenstrahlung from the Universe*, MPE Report 263, p. 9
- Lewin, W., van Paradijs, J., Taam, R. 1995, in W. Lewin, J. van Paradijs, E. van den Heuvel (eds.), *X-ray binaries*, Cambridge U.P., Cambridge, p. 175
- Margon, B., Bolte, M. 1987, *ApJ*, 321, L61
- Mattox, J., Bertsch, D., Chiang, J., et al. 1996, *ApJ*, 461, 396
- McGale, P., Pye, J., Hodgkin, S. 1996, *MNRAS*, 280, 627
- Monet, D., Bird, A., Canzian, B., et al. 1998, *The PMM USNO-A2.0 Catalog*, US Naval Observatory
- Perryman, M., Lindgren, L., Kovalevsky, J., et al. 1997, *A&A*, 323, L49
- Picard, A., Johnston, H. 1995, *A&AS*, 112, 89
- Trager, S., Djorgovski, S., King, I. 1993, in S. Djorgovski, G. Meylan (eds.), *Structure and Dynamics of Globular Clusters*, Vol. 50 of *ASP Conference Series*, ASP, p. 347
- Trümper, J., Hasinger, G., Aschenbach, B., et al. 1991, *Nat*, 349, 579
- Verbunt, F., Bunk, W., Hasinger, G., Johnston, H. 1995, *A&A*, 300, 732
- Verbunt, F., Bunk, W., Ritter, H., Pfeffermann, E. 1997, *A&A*, 327, 602
- Verbunt, F., Hasinger, G. 1998, *A&A*, 336, 895
- Verbunt, F., Meylan, G. 1988, *A&A*, 203, 297
- Verbunt, F., Shafer, R., Jansen, F., Arnaud, K., van Paradijs, J. 1988, *A&A*, 168, 169
- Vijapurkar, J., Drilling, J. 1993, *ApJS*, 89, 293
- Zimmermann, H., Becker, W., Belloni, T., Döbereiner, S., Izzo, C., Kahabka, P., Schwentker, O. 1996, *EXSAS User's Guide: Extended scientific analysis system to evaluate data from the astronomical X-ray satellite ROSAT*, Edition 5, Technical report, MPE